Epitaxial self-assembly of block copolymers on lithographically defined nanopatterned substrates

Sang Ouk Kim*†, Harun H. Solak‡, Mark P. Stoykovich*, Nicola J. Ferrier§, Juan J. de Pablo* & Paul F. Nealey*

** Department of Chemical Engineering and Center for Nanotechnology, and § Department of Mechanical Engineering, University of Wisconsin, Madison, Wisconsin 53706 USA*
‡ Laboratory for Micro- and Nanotechnology, Paul Scherrer Institute, CH-5232 Villigen PSI, Switzerland
† Present address: Samsung SDS Co. Ltd, 707-19, Yoksam-2 Dong, Kangnam-Gu, Seoul 135-918, Korea.

Parallel processes for patterning densely packed nanometre-scale structures are critical for many diverse areas of nanotechnology. Thin films of diblock copolymers[1–11] can self-assemble into ordered periodic structures at the molecular scale (~5 to 50 nm), and have been used as templates to fabricate quantum dots[1,2], nanowires[3–5], magnetic storage media[6], nanopores[7] and silicon capacitors[8]. Unfortunately, perfect periodic domain ordering can only be achieved over micrometre-scale areas at best[12,13] and defects exist at the edges of grain boundaries. These limitations preclude the use of block-copolymer lithography for many advanced applications[14]. Graphoepitaxy[12,15], in-plane electric fields[3,16], temperature gradients[17], and directional solidification[14,18] have also been demonstrated to induce orientation or long-range order with varying degrees of success. Here we demonstrate the integration of thin films of block copolymer with advanced lithographic techniques to induce epitaxial self-assembly of domains. The resulting patterns are defect-free, are oriented and registered with the underlying substrate and can be created over arbitrarily large areas. These structures are determined by the size and quality of the lithographically defined surface pattern rather than by the inherent limitations of the self-assembly process. Our results illustrate how hybrid strategies to nanofabrication allow for molecular level control in existing manufacturing processes.

In epitaxial assembly of block-copolymer films, molecular-level control over the precise size, shape and spacing of the ordered domains is achieved by specifying the volume fraction of each block and the length of the chains[19]. Lithographic patterning of surfaces provides the following desirable attributes of top-down fabrication techniques to our hybrid strategy: the ability to pattern over truly macroscopic areas, scalability and manufacturability, and placement of each domain, including registration and overlay, with nanometre precision. Epitaxial assembly contrasts with previous experimental studies that describe directed or guided assembly of lamellar domains on chemically striped substrates[20–22]. Even the highest-quality films in previous studies contained a high density of defects of unknown origin, and were quantified at best by a statistical degree of orientation[20]. Previous molecular simulation and theoretical studies also describe directed or guided orientation and ordering of cylindrical[23] and lamellar[24,25] domains on chemically nanopatterned substrates, but are limited in their predictive capabilities concerning epitaxial assembly owing to the finite size, periodic boundary conditions or reduced dimensionality of the analysis.

Figure 1 illustrates the two-step process used to prepare well-defined nanopatterned surfaces. Photoresist was patterned with alternating lines and spaces with periods between 45 and 55 nm using extreme ultraviolet interferometric lithography[26] (EUV-IL), and the pattern in the photoresist was transferred to an underlying self-assembled monolayer (SAM) by chemical modification of the SAM. The dimensions of the areas patterned with EUV-IL were approximately 50 μm by 400 μm, although the areas over which the patterns in the resist were perfect were smaller. The period of the chemical surface pattern was known from the design of the EUV-IL mask, and was confirmed by measuring the period of the patterned photoresist. Following removal of the remaining photoresist, a 60-nm film of symmetric lamella-forming poly(styrene-block-methyl methacrylate) ((PS-b-PMMA), 104 kg mol^{-1}, lamellar period approximately 48 nm) was spin-coated and annealed on the chemically patterned surface. The PMMA block preferentially wet the SAMs that were chemically modified to contain polar groups[27], and the other regions exhibited neutral wetting behaviour by the block copolymer. The domain structure of the block-copolymer film after annealing was imaged using scanning electron microscopy (SEM). The two-step process allows for unprecedented characterization of the chemically nanopatterned surfaces. Future applications may benefit from or require the synthesis of sensitive and chemically specific imaging layers that change functionality directly upon lithographic exposure.

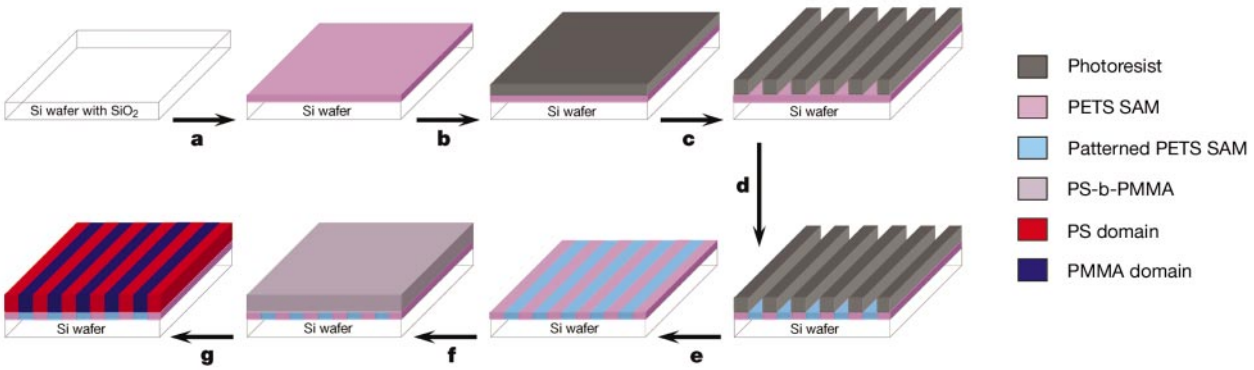

Figure 1 Schematic representation of the strategy used to create chemically nanopatterned surfaces and investigate the epitaxial assembly of block-copolymer domains. **a**, A SAM of PETS was deposited on a silicon wafer. **b**, Photoresist was spin-coated on the SAM-covered substrate, and **c**, patterned by EUV-IL with alternating lines and spaces of period L_s. **d**, The topographic pattern in the photoresist was converted to a chemical pattern on the surface of the SAM by irradiating the sample with soft X-rays in the presence of oxygen. **e**, The photoresist was then removed with repeated solvent washes. **f**, A symmetric, lamella-forming PS-b-PMMA copolymer of period L_0 was spin-coated onto the patterned SAM surface and **g**, annealed, resulting in surface-directed block-copolymer morphologies. Chemically modified regions of the surface presented polar groups containing oxygen and were preferentially wetted by the PMMA block, and unmodified regions exhibited neutral wetting behaviour by the block copolymer.

If the period of the chemically patterned SAM, L_s, was equal to the period of the lamellar spacing of the block copolymer, L_o, ($L_s = L_o = 48$ nm), then the lamellar domains in the block-copolymer films were oriented perpendicularly to the substrate and were perfectly registered with the chemical pattern of the SAM. The largest continuous area over which the chemical surface patterns were defect-free was larger than 8 μm by 5 μm. Figure 2a shows a representative top-down image of the registered and perfect long-range order of the overlying block-copolymer film over a 5 μm by 5 μm area. The longest linear distances over which the ordering of the block-copolymer film was perfect along a single lamellar domain (parallel to the pattern) and across the lamellar structure (perpendicular to the pattern) were approximately 400 and 50 μm, respectively, and corresponded to the dimensions of the patterned area.

We could correlate the defects in the ordering of the block-copolymer film, when they are present, directly to defects in the patterning of the photoresist and therefore to defects in the chemical pattern of the SAM. In our EUV-IL system, for example, reproducible fringes in the patterned photoresist appeared near the edges of the patterned area owing to diffraction effects. The defects consisted of stripes of slightly over- and underexposed material that diminished in intensity with distance from the edge of the patterned region (Fig. 2b). Defects in the domain structure of the block-copolymer films (Fig. 2c) occurred at the same locations as defects in the patterns of photoresist. In overexposed areas (see area (2) in Fig. 2b), the photoresist structures were discontinuous and lacked integrity. The structure of the block-copolymer film over these predominantly chemically modified and therefore polar regions (see area (2) in Fig. 2c) consisted of parallel lamellae with the PMMA block wetting the surface. In underexposed areas (see area (3) in Fig. 2b) the photoresist was not cleared completely between the patterned line structures and pattern transfer to the SAM did not occur. The structure of the block-copolymer film on these areas (see area (3) in Fig. 2c) consisted of unregistered perpendicular lamellae with no long-range order. This structure was consistent with that observed on unpatterned regions (see areas labelled (1) in Fig. 2b and c).

The natural grain size or length scale of ordering of lamellae, as observed on homogeneous neutral areas, was about $2L_o$. This length scale is significantly less than that in analogous sphere-forming and cylinder-forming block-copolymer films because of the reduced number of degrees of freedom available for the lamella-forming system to organize. Our approach, without optimization of interfacial interactions or processing conditions, resulted in registration and long-range ordering at length scales two to three orders of magnitude larger than the natural grain size. On the basis of these results, we believe that there is no inherent limitation on the size of the registered and ordered array of domains that can be created by epitaxial assembly on lithographically defined chemically nanopatterned substrates.

Distinctly different types of registration and ordering defects of lamellar domains were observed if L_s was slightly smaller or larger than L_o. Top-down images of the in-plane domain structure of PS-b-PMMA ($L_o = 48$ nm) and corresponding Fourier transform analysis of the images are shown in Fig. 3 for $L_s = 45$, 47.5, 50, 52.5 and 55 nm. The film thickness was 60 nm, or approximately $1.2L_o$, for all samples, and the images correspond to the best 3 μm by 3 μm area of the sample over which the chemical surface pattern was defect-free. For $L_s = 45$ nm, the lamellae were compressed but were for the most part registered and epitaxial to the surface pattern. The sharp peaks in the Fourier transform analysis correspond to a period of less than L_o. Occasionally the mismatch between $L_s < L_o$ led to the formation of pairs of defects.

For $L_s = 47.5$, $L_s \cong L_o$ and the registration and ordering of the block-copolymer domains was perfect over the entire imaged area. The Fourier transform analysis reveals only two very sharp peaks at

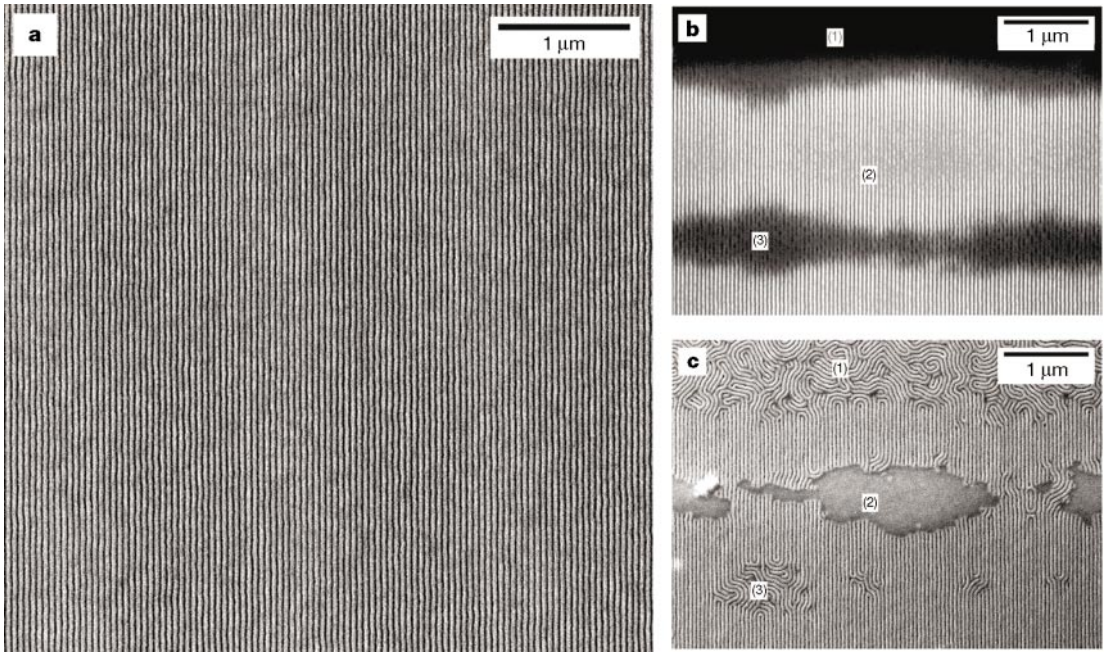

Figure 2 Top-down SEM images of photoresist and PS-b-PMMA copolymer ($L_o = 48$ nm, film thickness of 60 nm) patterns. In the SEM images of the PS-b-PMMA copolymer the light and dark regions were PS and PMMA domains, respectively. **a**, The perfect epitaxial ordering of a block-copolymer pattern extended over a 5 μm by 5 μm area. In this case, the SAM surface was chemically patterned with a period of $L_s = 47.5$ nm that matched L_o. **b**, Top-down SEM image of the photoresist pattern ($L_s = 47.5$ nm) at the edge of the region exposed using EUV-IL, and **c,** top-down SEM image of the morphology of a block-copolymer film overlying a chemically nanopatterned surface that was prepared (as in Fig. 1) using a photoresist pattern similar to that shown in **b**. To allow for comparison between samples, the exposure doses during EUV-IL and chemical modification steps were controlled to within 2%. Regions (1), (2) and (3) in **b** delineate unpatterned, overexposed, and underexposed areas of the photoresist, respectively. Regions (1), (2) and (3) in **c** show the block-copolymer morphologies observed over corresponding areas. Lamellae were oriented perpendicularly without long-range order on the unpatterned (1) and underexposed (3) regions. In the overexposed (2) regions the lamellae adopted a morphology that was parallel to the surface.

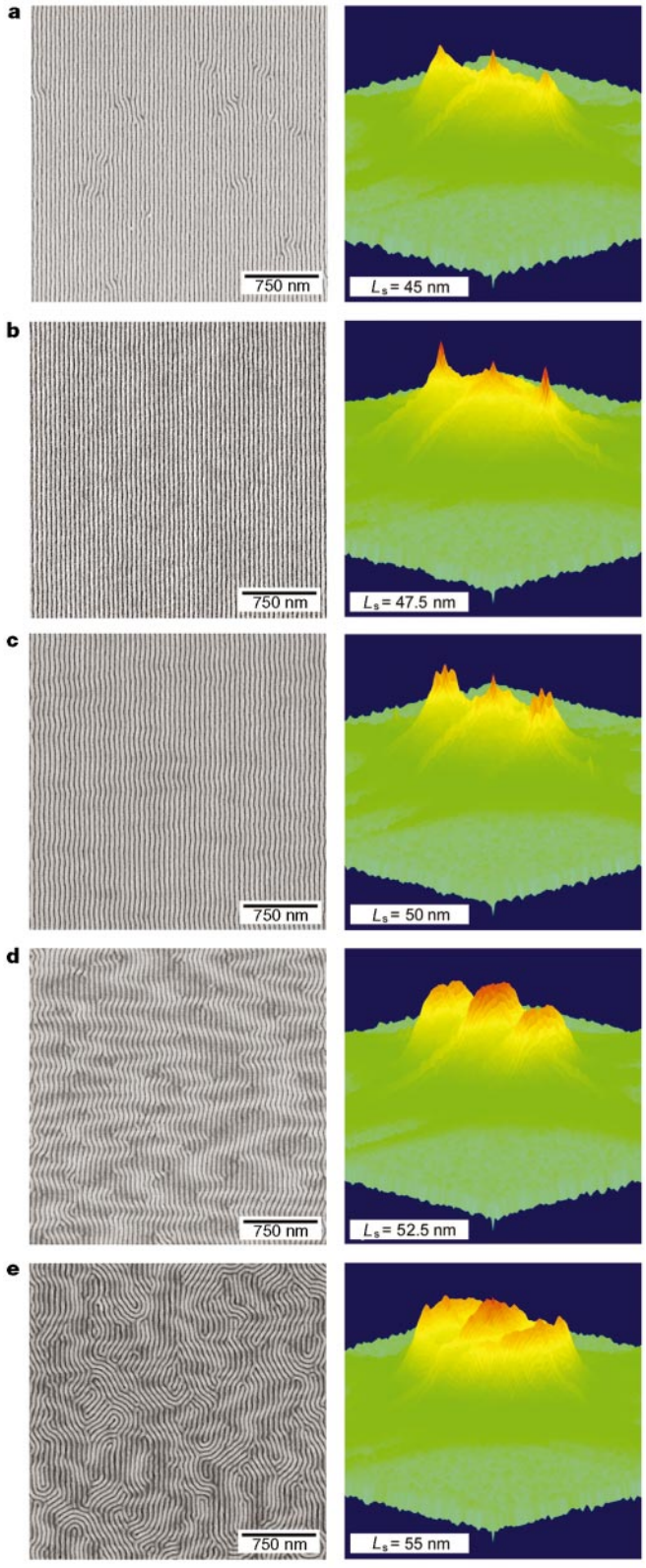

Figure 3 Top-down SEM images and corresponding Fourier transform analysis of PS-b-PMMA copolymer films (L_o = 48 nm, film thickness of 60 nm) on chemically nanopatterned surfaces. The surfaces had essentially perfect chemical patterns with periods, L_s, of: **a**, 45; **b**, 47.5; **c**, 50; **d**, 52.5; and **e**, 55 nm. The area of each SEM image corresponds to a 3 μm by 3 μm region of block-copolymer domains.

a characteristic period of 47.5 nm. For $L_s > L_o$, the top-down images revealed two distinct mechanisms of defect formation in the ordering of lamellar domains: (1) the formation of herringbone patterns and (2) unregistered lamellae with a period of L_o that were aligned to varying degrees with the axis of the surface pattern. As the difference between L_s and L_o increased, the angle between the herringbone pattern and the axis of the surface pattern, θ_{hb}, increased, and the fraction of lamellae registered and the degree of alignment of the unregistered lamellae with the surface pattern decreased. The herringbone morphology is particularly evident in the Fourier transform analysis of the sample with L_s = 50 nm. Six peaks appeared at periods in the neighborhood of L_o (Fig. 3c). The peaks associated with structures perpendicular to the axis of the surface pattern had a period slightly greater than L_o. The off-axis peaks corresponded to structures with a period of L_o, and the location of the peaks revealed a single value of $\theta_{hb} \approx 8°$. For L_s = 52.5 and 55 nm, the herringbone morphology was also observed but a much greater fraction of the lamellae fell out of registry with the surface pattern (Fig. 3d, e). In addition, multiple values of θ_{hb} were derived from the coordinates of local peaks in the Fourier transform analysis. For L_s = 55 nm, for example, the most intense peaks yielded values of θ_{hb} of ~10 and 25°.

Cross-sectional SEM images in Fig. 4 show that out-of-plane defects in ordering and orientation also occur for $L_s > L_o$. Lamellae are oriented perpendicular to the substrate for block-copolymer films on neutral homogenous (Fig. 4a) and for epitaxially ordered films if $L_s = L_o$ (Fig. 4b). The lamellae were tilted with respect to the surface normal, however, for films where $L_s > L_o$ (Fig. 4c). Tilt also introduces grain-boundary defects. Adoption of the herringbone and tilted morphologies are mechanisms by which the interfacial area between the PS and PMMA blocks and the polar stripes of the surface pattern are minimized and maximized, respectively. Consistent with the limitations of previously published models discussed earlier, tilted lamellae have been predicted by molecular

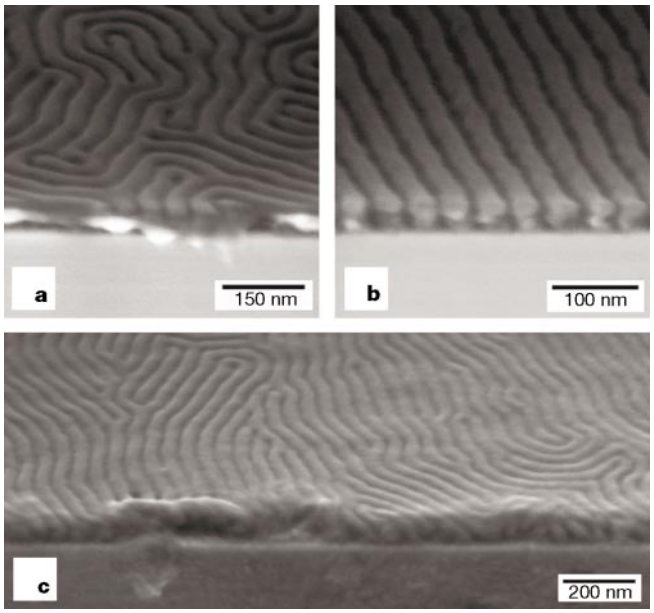

Figure 4 Cross-sectional SEM images of PS-b-PMMA films (L_o = 48 nm, thickness 60 nm) on unpatterned and chemically nanopatterned surfaces. The samples were cleaved under cryogenic conditions and imaging was performed on a stage tilted at 60°. **a**, Lamellae were oriented perpendicularly with no long-range order on unpatterned regions of the surface. **b**, Lamellae were oriented perpendicularly with epitaxial ordering on surfaces for which $L_s = L_o$. **c**, Lamellae exhibited both herringbone and tilt defects when the surface pattern (L_s = 55 nm) was greater than L_o.

simulation[24] and theory[25] but the herringbone morphologies have not.

These results clarify distinctions between epitaxial and surface-directed ordering of block-copolymer films. Orientation, registration and defect-free order required commensurability between the period of the surface pattern and the block copolymer within just a few per cent. If the periods of the surface and block copolymer agreed within approximately 10% ($L_s = 45$, 50 and 52.5 nm), the morphology of the block-copolymer film was surface-directed but not perfect. This constraint is a function of many parameters, including the polymer chemistry, film thickness and the magnitude of the surface and interfacial interactions.

There are essential aspects of this integrated fabrication strategy combining advanced lithography and self-assembly that enhance its potential technological impact. It is not limited to the use of PS-b-PMMA, but is applicable to other systems provided sufficient contrast can be achieved in the interfacial interactions between the patterned substrates and the blocks of the copolymer. Lithographic patterning of the substrate is simplified because the two-dimensional projections of desired domain structures in ordered block-copolymer films correspond to diffraction patterns that can be produced with multiple beam interferometry. Epitaxial assembly can easily be extended to cylinder-forming block copolymers that present immediate opportunities for the fabrication of addressable arrays for applications such as magnetic storage media. □

Methods

A SAM was deposited on a silicon wafer by immersing the sample in a 0.1 vol.% solution of phenylethyltrichlorosilane (PETS) in toluene for 1 h. A ~55-nm film of photoresist (PMMA, 960 kg mol^{-1}) was then spin-coated on the SAM-covered substrate and baked at 160 °C for 1 min to remove residual solvent. The PMMA was patterned using EUV-IL ($\lambda = 13.4$ nm, Center for NanoTechnology (CNTech), University of Wisconsin) in which achromatic radiation passed through a transmission membrane mask that consisted of a rectangular (~50 μm by 400 μm) opaque region, with grating structures of period p on opposing sides of the opaque region. The mask was fabricated by patterning chrome on a SiN membrane using electron beam lithography and reactive ion etching techniques. The first-order diffracted beams from the gratings interfere with one another in the shadow of the opaque region of the mask to generate an interference pattern with a period of $p/2$. We targeted 45 to 55 nm period lines and spaces, so the periods of the grating structures written on the mask were 90 to 110 nm. The gap between the mask and the sample was typically 0.35 mm, and the exposure tool offers exceptional depth of focus. After exposure, the PMMA was developed using standard lithographic procedures and blown dry in a stream of N_2. The period of the photoresist pattern was determined from SEM images by averaging over ten periods of lines. The topographic pattern in the photoresist was transferred to a chemical pattern on the surface of the SAM by irradiating the sample with soft X-rays ($\lambda = 1.1$ nm, ES-1 beamline at the CNTech) in the presence of oxygen (1 torr of air). The SAM in regions that were not covered by photoresist underwent photoelectron-induced reactions that led to the incorporation of polar, oxygen-containing functional groups on the surface. The remaining PMMA photoresist was stripped from the sample using chlorobenzene. Films of controlled thickness (~60 nm) of PS-b-PMMA (104 kg mol^{-1}, lamellar period of 48 nm) were deposited on chemically patterned substrates via spin-coating from dilute solutions in toluene. The films were then annealed for over 7 days at 190 °C. After annealing the domain structure of the block-copolymer film was imaged using a LEO 1550 VP field emission SEM.

Received 2 March; accepted 30 May 2003; doi:10.1038/nature01775.

1. Park, M., Harrison, C., Chaikin, P. M., Register, R. A. & Adamson, D. H. Block copolymer lithography: periodic arrays of ~10^{11} holes in 1 square centimeter. *Science* **276,** 1401–1404 (1997).
2. Li, R. R. *et al.* Dense arrays of ordered GaAs nanostructures by selective area growth on substrates patterned by block copolymer lithography. *Appl. Phys. Lett.* **76,** 1689–1691 (2000).
3. Thurn-Albrecht, T. *et al.* Ultrahigh-density nanowire arrays grown in self-assembled diblock copolymer templates. *Science* **290,** 2126–2129 (2000).
4. Kim, H. C. *et al.* A route to nanoscopic SiO_2 posts via block copolymer templates. *Adv. Mater.* **13,** 795–797 (2001).
5. Lopes, W. A. & Jaeger, H. M. Hierarchical self-assembly of metal nanostructures on diblock copolymer scaffolds. *Nature* **414,** 735–738 (2001).
6. Cheng, J. Y. *et al.* Formation of a cobalt magnetic dot array via block copolymer lithography. *Adv. Mater.* **13,** 1174–1178 (2001).
7. Chan, V. Z.-H. *et al.* Ordered bicontinuous nanoporous and nanorelief ceramic films from self assembling polymer precursors. *Science* **286,** 1716–1719 (1999).
8. Black, C. T. *et al.* Integration of self-assembled diblock copolymers for semiconductor capacitor fabrication. *Appl. Phys. Lett.* **79,** 409–411 (2001).
9. Fasolka, M. J. & Mayes, A. M. Block copolymer thin films: physics and applications. *Annu. Rev. Mater. Res.* **31,** 323–355 (2001).
10. Mansky, P., Liu, Y., Huang, E., Russell, T. P. & Hawker, C. Controlling polymer-surface interactions with random copolymer brushes. *Science* **275,** 1458–1460 (1997).
11. Huang, E., Rockford, L., Russell, T. P. & Hawker, C. J. Nanodomain control in copolymer thin films. *Nature* **395,** 757–758 (1998).
12. Segalman, R. A., Yokoyama, H. & Kramer, E. J. Graphoepitaxy of spherical domain block copolymer films. *Adv. Mater.* **13,** 1152–1155 (2001).
13. Harrison, C. *et al.* Mechanisms of ordering in striped patterns. *Science* **290,** 1558–1560 (2000).
14. Rosa, C. D., Park, C., Thomas, E. L. & Lotz, B. Microdomain patterns from directional eutectic solidification and epitaxy. *Nature* **405,** 433–437 (2000).
15. Cheng, J. Y., Ross, C. A., Thomas, E. L., Smith, H. I. & Vansco, G. J. Fabrication of nanostructures with long-range order using block copolymer lithography. *Appl. Phys. Lett.* **81,** 3657–3659 (2002).
16. Morkved, T. L. *et al.* Local control of microdomain orientation in diblock copolymer thin films with electric fields. *Science* **273,** 931–933 (1996).
17. Bodycomb, J., Funaki, Y., Kimishima, K. & Hashimoto, T. Single-grain lamellar microdomain from a diblock copolymer. *Macromolecules* **32,** 2075–2077 (1999).
18. Park, C. *et al.* Double textured cylindrical block copolymer domains via directional solidification on a topographically patterned substrate. *Appl. Phys. Lett.* **79,** 848–850 (2001).
19. Bates, F. S. & Fedrickson, G. H. Block copolymer thermodynamics: theory and experiment. *Annu. Rev. Phys. Chem.* **41,** 525–557 (1990).
20. Rockford, L. *et al.* Polymers on nanoperiodic, heterogeneous surfaces. *Phys. Rev. Lett.* **82,** 2602–2605 (1999).
21. Yang, X. M., Peters, R. D., Nealey, P. F., Solak, H. H. & Cerrina, F. Guided self-assembly of symmetric diblock copolymer films on chemically nanopatterned substrates. *Macromolecules* **33,** 9575–9582 (2000).
22. Rockford, L., Mochrie, S. G. J. & Russell, T. P. Propagation of nanopatterned substrate templated ordering of block copolymers in thick films. *Macromolecules* **34,** 1487–1492 (2001).
23. Wang, Q., Nealey, P. F. & de Pablo, J. J. Simulations of the morphology of cylinder-forming asymmetric diblock copolymer thin films on nanopatterned substrates. *Macromolecules* **36,** 1731–1740 (2003).
24. Wang, Q., Nath, S. K., Graham, M. D., Nealey, P. F. & de Pablo, J. J. Symmetric diblock copolymer thin films confined between homogeneous and patterned surfaces: Simulation and theory. *J. Chem. Phys.* **112,** 9996–10010 (2000).
25. Petera, D. & Muthukumar, M. Self-consistent field theory of diblock copolymer melts at patterned surfaces. *J. Chem. Phys.* **109,** 5101–5107 (1998).
26. Solak, H. H. *et al.* Sub-50 nm period patterns with EUV interference lithography. *Microelectron. Eng.* **67–8,** 56–62 (2003).
27. Dulcey, C. S. *et al.* Photochemistry and patterning of self-assembled monolayer films containing aromatic hydrocarbon functional groups. *Langmuir* **12,** 1638–1650 (1996).

Acknowledgements We thank F. Cerrina, E. W. Edwards and S. Xiao for discussions, and V. Golovkina and J. Wallace for assistance with the EUV-IL system. This work was supported by the Semiconductor Research Corporation, the National Science Foundation through the Materials Research Science and Engineering Center, and the Camille Dreyfus Teacher-Scholar Award. S.K. acknowledges a research fellowship from the Post-Doctoral Fellowship Program of the Korea Science and Engineering Foundation. Facilities and staff of the CNTech were supported by DARPA and the Intel Corporation, and the Synchrotron Radiation Center is supported by the National Science Foundation.

Competing interests statement The authors declare that they have no competing financial interests.

Correspondence and requests for materials should be addressed to P.F.N. (nealey@engr.wisc.edu).

Carbon solubility in olivine and the mode of carbon storage in the Earth's mantle

Hans Keppler*, Michael Wiedenbeck† & Svyatoslav S. Shcheka*

** Institut für Geowissenschaften, Universität Tübingen, Wilhelmstrasse 56, 72074 Tübingen, Germany*
† GeoForschungsZentrum Potsdam, ProjektBereich 4.2, Telegrafenberg, 14473 Potsdam, Germany

The total amount of carbon in the atmosphere, oceans and other near-surface reservoirs is thought to be negligible compared to that stored in the Earth's mantle[1–3]. Although the mode of carbon storage in the mantle is largely unknown, observations of microbubbles on dislocations in minerals from mantle xenoliths has led to the suggestion that carbon may be soluble in silicates at high pressure[4,5]. Here we report measurements of carbon solubility in olivine, the major constituent of the upper mantle, at pressures up to 3.5 GPa. We have found that, contrary to previous

